Comparative NEXAFS Study on Soot Obtained from an Ethylene/Air Flame, a Diesel Engine, and Graphite

Stefano di Stasio*,† and Artur Braun‡

Aerosol and Nanostructures Laboratory, Istituto Motori, CNR, Napoli, Italy, and Department of Chemical and Materials Engineering and Consortium for Fossil Fuel Science, University of Kentucky, Lexington, Kentucky 40515

Received June 7, 2005. Revised Manuscript Received October 6, 2005

Microstructure and molecular structure properties of different carbonaceous byproducts from combustion are fundamental to evaluate the radiative properties of such materials when combustion aerosols interact with solar radiation in atmosphere. Carbon near edge X-ray absorption fine structure (NEXAFS) spectroscopy is presented as an analytical technique for the carbon-specific characterization of various soot species. Ethylene soot, diesel soot, and carbon black NEXAFS spectra are discussed in relation to graphite as the most genuine model compounds of soot. Characteristic resonances in the spectra allow for the direct molecular speciation of the graphite-like solid core in soot, surface functional groups, and aromatic and aliphatic components, depending on the origin of the soot. Moreover, in the experimental case of ethylene soot samples probed at increasing distances from the burner nozzle, namely, at increasing residence times, NEXAFS experiments lead to the evidence that the soot collected near the nozzle appears to be more graphitized than soot sampled at larger heights-above-burner, in qualitative agreement with laser light scattering depolarization measurements reported here and previous findings obtained by electron microscopy characterization. The possible implications of the presented results on soot formation mechanism, combustion source attribution of carbon particulates, and UV−vis sunlight absorption by black carbon aerosols are briefly discussed.

1. Introduction

Soot represents the residual material obtained from combustion of biomass, coal, and diesel fuel. It includes both elemental carbon (EC) and organic carbon (OC) compounds. About elemental analysis, soot represents a complex mixture of carbon and hydrogen with traces of other species depending on the particular combustion process. For instance, soot from flames generally contains at least 1 wt % of hydrogen, which corresponds, on an atomic basis, approximately to the empirical form C_8H.[1]

Carbonaceous powders produced by controlled thermal decomposition or partial combustion of hydrocarbons are known as *carbon blacks*. Different types of carbon blacks can be produced by different industrial processes, including acetylene black, channel black, furnace black, lamp black, and thermal black. Carbon blacks are used as ink, paints, rubber, and filler material in the tire industry.

The term *black carbon* (BC) describes "combustion derived black particulate carbon having a graphitic microstructure".[2] BC is present in air, soils, ices, snow, and rain, and it is characterized by chemical inertness with respect to environmental degradation processes.

Carbonaceous aerosols released in the troposphere are thought to be co-responsible for the earth global warming processes[3] in that they absorb ultraviolet and visible sunlight. A peculiar characteristic of BC aerosols different from other gaseous atmospheric pollutants, such as CO_2, is to be characterized by concentration that varies dramatically with location. Consequently, the knowledge of the relative BC abundance is crucial in the prediction of climatic changes in regional areas where anthropogenic (smoke emissions) or natural events (forest fires, volcano eruptions) eventually occur.

Soot fine powders can be characterized on a structural basis by several molecular arrangements, which span from amorphous to layered stacked lattice (graphite-like). When interaction of carbonaceous aerosols with solar radiation is considered, the different structures reflect different absorbing properties, especially at UV side of the spectrum. In particular, the so-called soot *graphitization* process (i.e., the creation at high temperatures of ordered lattice planes of stacked carbon atoms) yields to the shift of the absorption peak observed for soot at about 220 nm to longer wavelengths.[4] The radiative properties of carbon particles with respect to sunlight, particularly the complex refractive index $m = n + ik$, can be evaluated with simple optical dispersion models, such as the Drude−Lorentz scheme.[5] The values of (n,k) are strongly conditioned by several parameters, such as the free electron concentration, which drastically changes in correspondence of carbon types with different amount of microstructural local order.

Therefore, in the framework of climate change, it is important to distinguish between different types of soot and carbon byproducts from different combustion processes both to predict the radiative transfer and to attribute the fossil fuel burning

* Corresponding author. Phone: ++39 81 71 77 122. Fax: ++39 81 239 60 97. E-mail: s.distasio@im.cnr.it.
† Istituto Motori, CNR.
‡ University of Kentucky.

(1) Palmer, H. B.; Cullins, C. F. In *The Chemistry and Physics of Carbon*; Walker, P. L., Ed.; Dekker: New York, 1965; Vol. 1, p 265.
(2) Novakov, T. *Sci. Total Environ.* **1984**, *36*, 225−234.
(3) Chameides, W. L.; Bergin, M. *Science* **2002**, *297*, 2214−2215.
(4) Kimura, Y.; Sato, T.; Kaito, C. *Carbon* **2004**, *42*, 33−38.
(5) Bohren, C. F.; Huffman, D. R. *Absorption and Scattering of Light by Small Particles*; Wiley: New York, 1983.

10.1021/ef058019g CCC: $33.50 © 2006 American Chemical Society
Published on Web 11/15/2005

sources. It should be stressed that the different structural properties, particularly the degree of graphitization as discussed above, are expected to influence the adsorption process of gaseous pollutants on the particulate suspended in the atmosphere.[6]

Soot formation process is governed by complexity. The deep understanding of this mechanism embraces knowledge of thermodynamics, cluster physics, chemistry, and kinetics. The ordinary scheme that is presented in the literature for low-pressure flames is that soot nuclei are formed via polycyclic aromatic hydrocarbons[7] by a process usually called nucleation or inception that converts mass from molecular to particulate regime. Thus, the formation of the first aromatic rings is followed by the growth by addition of C_1H_m or C_2H_n molecules. Acetylene is suggested to be the main building block. Reactive polyaromatic hydrocarbon (PAH) coagulation is advocated to explain the formation of larger PAHs.[8,9] The collision diameter of these heavy PAHs is known to be about 1.5−2.0 nm,[10] and the mass about 2000 amu. Chemical details of this process are still a challenge because chemical measurements of gas phase and particle phase are difficult to be performed concurrently. For instance, gas chromatography and mass spectrometry are not able to follow molecular mass larger than about 800 amu, and the radiation damages in electron energy loss spectroscopy (EELS) can significantly alter the sample before critical information on the sample is gathered. This holds particularly true for EELS with very high accelerator voltages in connection with electron microscopes.[11]

After the formation of nuclei, mass is believed to grow through the addition of gas-phase species such as acetylene and small PAHs and contemporary reactive coagulation via particle−particle collisions. Soot precursors are referred to as transparent particles and have been observed by ex situ sampling and transmission electron microscopy (TEM) analysis[12−14] and in situ optical experiments[15,16] or by a combination of in situ and ex situ diagnostics.[17]

At higher residence times a process is usually believed to dominate, which is termed *carbonization* and consists of functional group elimination, ring condensation and fusion, transformation of aliphatic chains into aromatic rings, and alignment of polyaromatic layers. From an elemental point of view this translated as dehydrogenation process, which converts the amorphous polyaromatic carbon to progressively graphitic material. This process of partial microstructure ordering can yield some decrease in particle mass.

Soot precursors[18] are thought to be of relatively low density (∼1.2 g/cm^3), with a C/H ratio of approximately 2 and optical nonabsorbing in the visible, namely with imaginary part k of refractive index $m = n + ik$ about zero, whereas more graphitic carbon matter is found to have higher density (∼1.8−2.0 g/cm^3) with a C/H ratio 6−8 and with an high k in the visible in the range 0.4−1.0. Simple models of the optical constant[5,19−21] demonstrate that the lower is the H/C ratio, the higher is the absorption index k, owing to the influence exerted on the optical properties by the free electron concentration.

Relatively recent works based on more sophisticated experimental techniques complicate the above expected framework. Different articles focus on the carbonization process.

Laser microprobe mass spectrometry and combined TEM analysis[22] were used to study the evolution of soot precursor particles to carbonaceous aggregates in a laminar ethene diffusion flame. Carbonization was observed on the center line of the flame during the abrupt change of single precursor liquidlike particles to fused aggregates at a narrow range of heights-above-burner between 30 and 40 mm. This mechanism was found to correspond to a quick decrease in the hydrogen mole fraction from 0.35 to 0.15.

Other authors[23] revealed the carbonization process in a laminar ethylene/air diffusion flame by using the signal from laser-induced fluorescence and laser-induced incandescence to distinguish the presence of PAHs and soot containing particles, respectively. Bright and dark field TEM was then used to track the carbonization process, namely, the transition from soot precursors to carbonaceous soot with increasing crystallinity (i.e., increasing relative abundance of graphitic crystallites). Consistent with previous literature from carbon black studies,[1,24] each crystallite was thought to consist of 5−10 sheets of carbon atom with external size about 2−3 nm.

Real time ex situ aerosol mass spectrometry was applied to observe the carbonization process in an acetylene diffusion flame.[25] Size distributions of PAH-containing and mature soot particles were measured. Very large PAHs were observed to form as a consequence of a rapid exchange of hydrogen and the pyrolytic addition of small hydrocarbons. Those authors proposed that the carbonization occurs in some milliseconds by transformation of very large (several hundred nanometers) droplets through nucleation sites formed directly at the droplet surface by dehydrogenation and molecular weight growth. These nuclei are proposed to grow in size from the surrounding PAHs and concurrently to interact via van der Waals forces to form the fractal aggregates characteristic of mature soot corresponding to the stage when all the PAHs have been carbonized.

Other authors[26] investigated the correlation between internal structure and spectral behavior of carbon blacks produced by electrical heating of graphite electrodes and condensation by cooling in He, Ar, Ar/H_2, and pure H_2 atmospheres at pressures ranging from 10 to 100 mbar. Internal structure of particles was studied by high-resolution TEM, EELS, nuclear magnetic resonance (NMR), and Raman spectroscopy. Primary particles were observed to consist of bent or plane basic structural units (BSUs) constituted by 4−5 graphene layers stacked together,

(6) Kandas, A. W.; Gokhan Senel, I.; Levendis, Y.; Sarofim, A. F. *Carbon* **2005**, *43*, 241−251.
(7) Richter, H.; Howard, J. B. *Prog. Energy Combust. Sci.* **2000**, *26*, 565−608.
(8) McKinnon, H. *Proc. Combust. Inst.* **1992**, *24*, 965−971.
(9) Hepp, H.; Siegmann, K.; Sattler, K. *Chem. Phys. Lett.* **1995**, *233*, 16−22.
(10) Wang, H.; Frenklach, M. *Combust. Flame* **1994**, *96*, 163−170.
(11) Braun, A.; Huggins, F. E.; Shah, N.; Chen, Y.; Wirick, S.; Mun, S. B.; Jacobsen, C.; Huffman, G. *Carbon* **2005**, *43*, 117−124.
(12) Megaridis, C. M.; Dobbins, R. A. *Combust. Sci. Technol.* **1989**, *66*, 1−16.
(13) Vander Wal, R. *Combust. Sci. Technol.* **1997**, *126*, 333−357.
(14) di Stasio, S. *Carbon* **2001**, *39*, 109−118.
(15) D'Alessio, A. *Proc. Combust. Inst.* **1992**, *24*, 973−980.
(16) Minutolo, P.; Gambi, G.; Dalessio, A.; Danna, A. *Combust. Sci. Technol.* **1994**, *101*, 311−325.
(17) Sgro, L. A.; Basile, G.; Barone, A. C.; D'Anna, A.; Minutolo, P.; Borghese, A.; D'Alessio, A. *Chemosphere* **2003**, *51*, 1079−1090.
(18) Dobbins, R. A. *Combust. Flame* **2002**, *130*, 204−214.
(19) Dalzell, W. H.; Sarofim, A. F. *J. Heat Transfer* **1969**, *91*, 100−104.
(20) Lee, S. C.; Tien, C. L. *Proc. Combust. Inst.* **1981**, 1159−1166.
(21) di Stasio, S.; Massoli, P. *Meas. Sci. Technol.* **1994**, *5*, 1453−1465.
(22) Dobbins, R. A.; Fletcher, R. A.; Chang, H.-C. *Combust. Flame* **1998**, *115*, 285−298.
(23) Vander Wal, R. L. *Combust. Flame* **1998**, *112*, 607−616.
(24) Siegla, D. C., Smith, G. W., Eds. *Particulate Carbon*; Plenum: New York, 1981.
(25) Reilly, P. T. A.; Gieray, R. A.; Whitten, W. B.; Ramsey, J. M. *Combust. Flame* **2000**, *122*, 90−104.
(26) Jäger, C.; Henning, Th.; Schloegl, R.; Spillecke, O. *J. Non-Cryst. Solids* **1999**, *258*, 161−179.

onionlike or amorphous, depending on the species and pressure of the quenching gas. Moreover, the degree of curvature of graphene layers or BSUs was found to depend on the particle size and from one location to the other within each primary particle. Thus, those authors used the EELS results to obtain a quantitative structural analysis. The core-loss transitions corresponding to electron transition from the K-shell C(1s) to energy levels above the Fermi level were investigated, in particular at 286 and 290 eV, and used to distinguish the sp^2 and sp^3 hybridization states of carbon. The method was based on the assumption that the integral intensity of electron transitions for π- and σ-electrons was proportional to the number of the effective π- and σ-bondings in the carbon sample, consistent with findings by other authors.[27,28] In this way, the bent graphene layers were characterized in terms of the sp^2/sp^3 ratio, which was compared to the 100% sp^2 standard graphite sample constituted of randomly oriented graphitic regions and used as a parameter to discriminate the more or less graphitic character.

Wentzel et al.[29] studied size, morphology, and microstructure of standard generated soot (spark discharge Palas soot), diesel soot, and diesel soot/ammonium sulfate mixtures. Diesel soot was observed to exhibit an onion-shell structure with graphite domain size about 2−3 nm. Fractal dimension of particles was derived by TEM images and predicted by aerosol dynamic simulations.

Ishiguro et al.[30] reported the observation of inner core and outer shell in diesel soot primary particles by phase-contrast and hollow-cone beam methods of operating TEM. The microstructure of inner core (diameter $\approx$ 10 nm) was observed to be constituted by several fine particles about 3−4 nm size, and in turn, each fine particle was characterized by a nucleus about 1 nm covered by carbon layers with distorted structure.

From the aforementioned, it is evident that a better comprehension of the microstructure of particulate obtained from combustors burning different fuels and/or from the same burner fuel system at different stages of carbonization and oxidation processes would be necessary.

X-ray absorption techniques represent a valuable tool in characterization of local microstructural order of BC in that the absorption spectra significantly depend on the way locally the atoms are bonded to neighboring atoms. In particular, the near-edge X-ray absorption fine structure (NEXAFS) spectrum characterizes the absorption of carbonaceous matter around the so-called carbon K-shell absorption edge at about 285 eV (wavelength of incident X-radiation 4.35 nm) depending on different electron transition.

The aim of the present article is to study with NEXAFS and laser light depolarization techniques different types of soot (ethylene/air flame, diesel engine), carbon black, and graphite.

The NEXAFS spectroscopy compared to the EELS and ultra-small-angle X-ray scattering have been used in our previous work to investigate diesel soot.[11,31] Since NEXAFS is a relatively novel technique, it is still difficult at this time for a fair and final comparison with related techniques such as electron-, Raman-, and infrared spectroscopy, but a critical review on NEXAFS for carbon materials was published recently.[32] Here, NEXAFS spectroscopy is used to study ethylene/air soot and other solid carbonaceous materials such as graphite, diesel soot, and carbon black in terms of molecular structure and surface functional groups. Soot from different distances from the burner nozzle experiences an external environment with different oxygen concentration and hence has a different extent of surface functional groups. The results from NEXAFS are discussed and compared with the findings from light scattering experiments measuring the depolarized light intensity by the soot in the flame. X-ray absorption and laser light depolarization results do correspond to make focus on the short-range ordering of soot local microstructure.

The microstructure, and in particular the graphitization degree, is demonstrated to characterize each sample, being useful as a fingerprint to attribute combustion history of particulate. The consequences of such findings with respect to the mechanism of UV sunlight absorption by differently structured soots are discussed with concern to the radiative forcing balance in the atmosphere on regional scale.

2. Experimental Section

Ethylene soot was obtained from an ethylene/air diffusion flame (Bunsen burner) with an ethylene flow rate of 14 cm^3/s. The length of the flame was 17 cm. Samples were collected at 20, 40, and 70 mm distance from the burner nozzle. The diesel soot studied here is NIST SRM 1650, purchased from the U.S. National Institute of Standards and Technology (NIST) in Gaithersburg, MD.[33] The carbon black sample is from the type N299.[34] The graphite is from the type LS25. Particle sizes of ethylene soot were obtained with SEM. Light scattering was used to determine the depolarization of soot. The experimental setup to perform the measurements of depolarized laser light scattering and the methodology for sampling soot primary particles and SEM analysis are fully described in previous work.[35,36] Soot is obtained at atmospheric pressure by using a Bunsen burner, inner diameter 1 cm, fueled with bottled ethylene (purity better than 99.95%) with a cold gas flow rate 11 cm^3/s. The height of the visible flame is about 17 cm.

The aforementioned samples were subject to carbon K-edge NEXAFS at Beamline 9.3.2 at the Advanced Light Source (ALS) at Lawrence Berkeley National Laboratory in Berkeley, CA.

For better handling during experiments, samples were pressed into pellets at 24 000 lb and mounted on a stainless steel sample holder. Using a load lock, we transferred samples to an ultrahigh vacuum recipient with a typical pressure of 2.5×10^{-10} mbar. The synchrotron storage ring was operated at 2.1 GeV. The resolving power of the monochromator grating was typically $E/\Delta E = 6000$, resulting in an energy resolution of approximately 0.05 eV for the relevant carbon K-shell absorption edge energy (285 eV). The incident beam intensity was recorded with a gold mesh reference monitor (I_o), and the NEXAFS signal of the sample was detected in both total electron yield (TEY) modus and sample current (SC) modus. For every sample, three scans ranging from 260 to 400 eV were made with energy steps of 0.1 eV. The NEXAFS spectra were obtained by forming the ratio I_{SC}/I_o for the sample current mode and $(I_{TEY}/I_o)/(I_{Au}/I_o)$ for the electron yield mode, with I_{Au}/I_o as the signal taken from a clean gold surface.

For quantitative analysis, the ethylene soot spectra were normalized to unity at 292 eV. For data reduction and quantitative analysis, the program WinXAS[37] was used.

(27) Madakson, P.; Nunes, S.; Galligan, E.; McGouey, R.; Chou, N. *Nucl. Instrum. Methods Phys. Res., Sect. B* **1990**, *45*, 216−218.
(28) Bruley, J.; Madakson, P.; Liu, J. C. *Nucl. Instrum. Methods Phys. Res., Sect. B* **1990**, *45*, 618−621.
(29) Wentzel, M.; Gorzawski, H.; Naumann, K.-H.; Saathoff, H.; Weinbruch, S. *J. Aerosol Sci*. **2003**, *34*, 1347−1370.
(30) Ishiguro, T.; Takatori, Y.; Akihama, K. *Combust. Flame* **1997**, *108*, 231−234.
(31) Braun, A.; Huggins, F. E.; Seifert, S.; Ilavsky, J.; Shah, N.; Kelly, K. E.; Sarofim, A.; Huffman, G. P. *Combust. Flame* **2004**, *137*, 63−72.
(32) Braun, A. *J. Environ. Monit.* **2005**, *7*, 1059−1065.
(33) Huggins, F. E.; Huffman, G. P.; Robertson, J. D. *J. Hazard. Mater*. **2000**, *74*, 1−23.
(34) Zerda, T. W.; Xu, W.; Yang, H.; Gerspacher, M. *Rubber Chem. Technol*. **1998**, *71*, 26−37.
(35) di Stasio, S. *Appl. Phys. B* **2000**, *70*, 635−643.
(36) di Stasio, S. *J. Quant. Spectrosc. Radiat. Transfer* **2002**, *73*, 423−432.

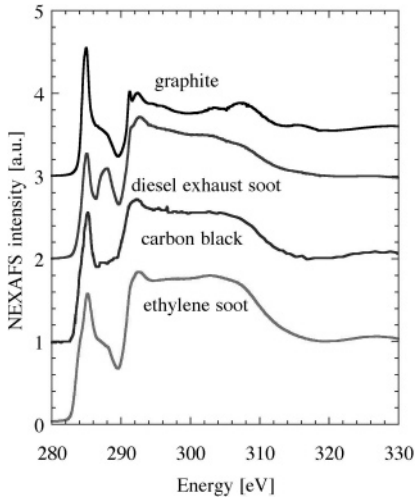

Figure 1. Carbon K-edge NEXAFS spectra of graphite LS 25, diesel soot NIST 1650, carbon black N299, and soot from atmospheric ethylene/air diffusion flame.

Table 1. Assignment of NEXAFS Peak Positions and Molecular Species (after Cody et al.[41])

energy (eV)	electronic transition	functionality
283.7	1s-π*	quinone
	1s-π*	protonated/alkylated
284.9−285.5		aromatic and PNA
	1s-π*	carbonyl substituted
285.8−286.4		aromatic, phenolic
	1s-π*	aromatic C−OH
		ketone-C═O
287.1−287.4		aliphatic
	1s-π*	aromatic carbonyl
287.7−288.3		C═O
287.6−288.2	1s − 3p/σ*	CH_3, CH_2, CH
288.2−288.6	1s-π*	COOH
289.3−289.5	1s-3p/σ*	C−OH, alcohol

Carbon black NEXAFS spectra were reproduced after data taken by Smith et al.[38] at the ALS. The NEXAFS of diesel fuel and lubricant oil were reproduced from an earlier study.[39]

3. Results and Discussion

3.1. Ethylene Soot versus Other Carbonaceous Samples. The background subtracted and normalized NEXAFS spectra of graphite, diesel soot, carbon black, and ethylene soot are displayed in Figure 1. For peak assignments, an earlier EELS study by Francis and Hitchcock[40] as well as a list recently published by Cody et al.[41] is helpful (the list is reproduced in Table 1). The graphite spectrum shows the pronounced π-peak at 285 eV and the corresponding σ-peak at 292 eV. These peaks arise from C═C bonds. The long-range order of graphite typically induces a sharp exciton peak at 291 eV.[42]

Confirmation of short-range order in the graphite comes from the extended X-ray absorption fine structure (EXAFS) oscillations in the spectrum for energies above 300 eV (maxima at 303.5, 307.5, and 315.5 eV).

Table 2. Peak Height Ratios I_π/I_σ

sample	graphite	ethylene soot	diesel soot	carbon black
I_π/I_σ	1.55	0.86	0.73	0.91

The intensity shoulder at 291 eV in the diesel soot spectrum can be interpreted as a tendency for the development of exciton. It appears that diesel soot also has some weak EXAFS oscillations in the same energy range and positions such as graphite. It is harder to make out such EXAFS oscillations for the carbon black and ethylene soot spectra. We thus conclude that diesel soot shows essentially higher order than ethylene soot or carbon black.

The ratio of peak heights for the C═C π-peak at 285 eV and the σ-peak at 292 eV is frequently used to quantify the degree of graphitization in carbonaceous materials, often in connection with EELS.[26] We show such results in Table 2. In graphite, the sharp peak dominates the entire spectrum, and the intensity ratio is 1.55. The NEXAFS spectra of all other samples presented here have ratios smaller than 1. The ratios are 0.91 for carbon black N299, 0.86 for ethylene soot, and 0.73 for the NIST SRM 1650 diesel soot.

According to the peak height ratios, diesel soot seems to be the least graphitized sample among the solid carbonaceous samples.

The primary peak at 285 eV arises from carbon atoms in homogeneous aromatic rings. If other atoms are attached to carbon in these rings, such as H, O, or groups such as −OH, and so forth, then electron charge is reorganized, which causes a chemical shift of the NEXAFS spectrum or occurrence of additional transitions. Due to this rearrangement of electrons, about 1 eV less in energy is required to excite an electron from a carbon atom in the aromatic ring from π- to an σ-level, which finds its manifestation in the resonance at 284 eV. The graphite has an overall full width at half-maximum intensity in this energy range smaller than that of the soot. This is not surprising because graphite has long-range order and a smaller surface/volume ratio than the soot, and the groups or atoms that cause rearrangement of electron charge are located at the surface.

The most striking difference between diesel soot and ethylene soot, as opposed to graphite, is an accumulation of peaks at 286.5−288.5 eV, which is due to phenol groups (286.5 eV), aliphatic side chains (287.3 eV), and carboxyl groups (288.4 eV). In all our studies thus far, we have not found a single diesel soot sample that did not show enhanced intensity at these energies.

Closer inspection of the diesel soot NEXAFS spectrum shows additional resonance peaks at 287 and 288 eV, which result from carbon atoms bonded in C−OH and COOH, and also C−H, respectively. Residual fuel and oil are most likely responsible for this signature in the diesel soot spectrum. Lubricant oil and diesel fuel have pronounced intensity in exactly this energy region.[39]

Figure 2 shows the NEXAFS spectra of oil and diesel, which both have minor intensity at 285 eV due to aromatically bound carbon in C═C, but significant intensity at 287 and 288 eV, which accounts most likely for the C−OH and C−H groups. The fuel spectrum has a higher peak at 285 eV than the oil spectrum.

We can assume that such groups are virtually absent on graphite. At least, they are not significantly present. The spectra presented here for the solid carbon material were obtained with the sample current NEXAFS detection mode, which is sensitive

(37) Ressler, T. *J. Synchrotron Radiat.* **1998**, *5*, 118−122.
(38) Smith, A. P.; Herd, C. R.; Magee, R. W.; Ade, H. Characterization of carbon black morphology in poorly dispersed rubber tire compounds by STXM. *Compendium of Abstracts*; Advanced Light Source: Berkeley, CA, 2002.
(39) Braun, A.; Shah, N.; Huggins, F. E.; Huffman, G. P.; Wirick, S.; Jacobsen, C.; Kelly, K.; Sarofim, A. *Fuel* **2004**, *83*, 997−1000.
(40) Francis, J. T.; Hitchcock, A. P. *J. Phys. Chem.* **1992**, *96*, 6598−6610.
(41) Cody, G. D.; Ade, H.; Wirick, S.; Mitchell, G. D.; Davis, A. *Org. Geochem.* **1998**, *28*, 441−455.
(42) Coffman, F. L.; Cao, R.; Pianetta, P. A.; Kapoor, S.; Kelly, M.; Terminello, J. L. *Appl. Phys. Lett.* **1996**, *69*, 568−570.

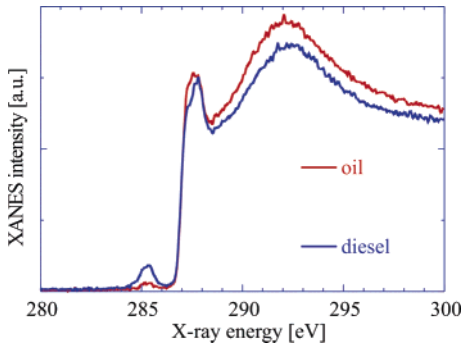

Figure 2. Carbon K-edge NEXAFS spectra lubricant oil Halvoline 10W30 (the higher intensity spectrum for $E > 287$ eV) and 50%/50% Philips T19 and Chevron U22 diesel fuel.

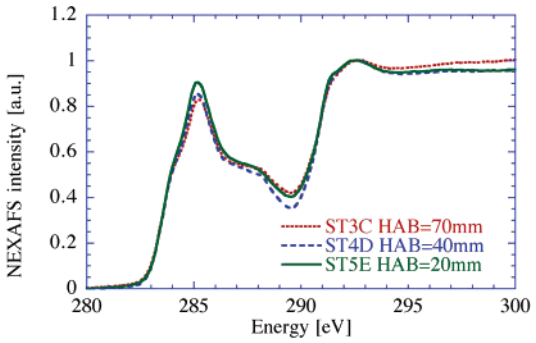

Figure 3. Carbon K-edge NEXAFS spectra of three ethylene soot samples. For better visual distinction of the spectra, sample heights in millimeter are given at maximum and minimum values of intensity.

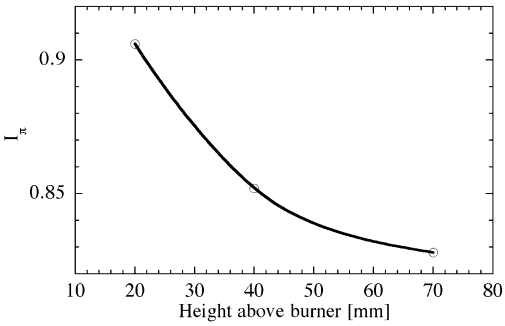

Figure 4. Intensity of the graphite peak maximum at 285 eV for the ethylene soot NEXAFS spectra as a function of height above burner. The solid line is a guide to the eye.

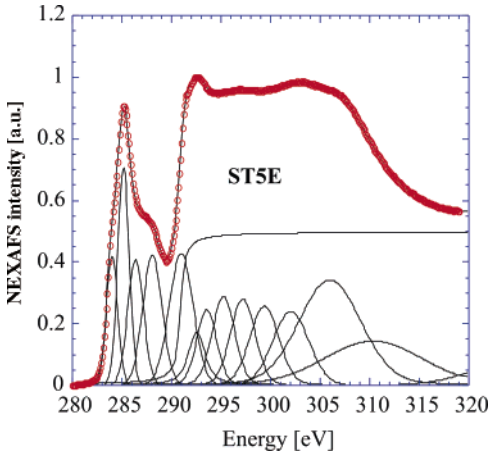

Figure 5. Carbon K-edge NEXAFS spectrum and peak assignment of ethylene soot, sampled at 20 mm from the burner nozzle.

for the bulk properties of the material. We have also acquired spectra with the total electron yield NEXAFS detection mode. This detection mode probes only electrons that come from the very 10−30 Å of the surface of the probed sample and hence is very surface-sensitive. By keeping in mind that the spectra presented here are bulk-sensitive, it is justified to say that both graphite and the ethylene soot contain no significant amount of C−OH and COOH groups.

Graphite, diesel soot, and ethylene soot have in common the pronounced dip at energies over 288 eV, with the minimum at 289.5 eV. Carbon black, however, does not have such a dip and hence could have significantly more C−H groups, which are typically found at 289 eV.

Finally, upon closer inspection of the ethylene soot spectrum, we find at around 284 eV a pronounced intensity shoulder, which we believe is due to benzoquinone. Benzoquinone is two C═O groups in an aromatic carbon ring. The resonance at around 284 eV comes from the carbon atoms in this ring, which are not bound to the oxygen atoms. The C═O groups in benzoquinone basically represent two carbonyl groups, which have their own characteristic resonance around 286 eV. The oxygen in the benzoquinone group causes a strong polarization of the electron cloud around the carbon atoms. The carbon atoms next to the oxygen experience a shift of the absorption edge toward higher X-ray energy (oxidation), while the remainders experience a shift toward energies lower than those observed in carbon atoms in a typical aromatic ring. Very close inspection of this energy region for all spectra shows that the ethylene soot has in fact a broadening of the peak at 285 eV in both directions, this is, toward 284 eV and toward 286 eV. From other studies, we know that diesel soot also contains benzoquinone, but not to the extent as observed here with the ethylene soot.[11]

3.2. Ethylene Soot for Various Sampling Heights. Let us turn now to the comparison of ethylene soot, sampled at three different distances from the burner nozzle. Compared to those of the previous samples (diesel soot, graphite, carbon black), the ethylene NEXAFS spectra, reported in Figure 3, basically look all the same.

Yet, minute differences are clearly visible. Since all spectra were normalized to unity at 292 eV, differences in intensity at the "graphite" peak at 285 eV are indicative of actual differences in the sample. It appears that the ratio of π-peak intensity and σ-peak intensity (arbitrarily set to unity for convenient analysis) is decreasing in sequence of sampling height 20, 40, and 70 mm, because the NEXAFS spectrum of the 20-mm sample has the highest and 70 mm has the lowest intensity at the graphite peak energy. We have plotted this ratio in Figure 4 as a function of the height above the burner nozzle. The striking result is that the sample with the higher intensity corresponds to the higher degree of graphitization or, in other words, the soot sampled at larger distances from the nozzle (larger residence times) is less graphitic. Samples with a higher degree of graphitization have larger graphite nanocrystallites and hence a lower surface-to-volume ratio. Since benzoquinone structures are only attributed to the boundary of aromatic ring arrangements, the benzoquinone peak intensity should relatively decrease when the graphite peak increases.

We have deconvoluted the spectra into mixed Gaussian and Lorentzian peaks with least-squares fitting, as shown in Figure 5. The peak assignment is not unambiguous in every energy region.

The first peak appears at 284 eV and is assigned to the benzoquinone groups. The next peak is due to the genuine aromatic C═C bonds of carbon in a graphite arrangement, at

Table 3. Area under the Peaks for Benzoquinone (First Peak), Graphite (Second Peak), after the Deconvolution in Figure 5

	benzoquinone	graphitic	benzoquinone+ graphitic	benzoquinone/ graphitic
70 mm	0.0142	0.0158	0.300	0.897
40 mm	0.0151	0.0178	0.330	0.852
20 mm	0.0146	0.0200	0.345	0.729

285 eV. Two more peaks covering the energy range from 286.5 to 288.5 eV are necessary to account for the measured NEXAFS intensity. The first of these peaks can account for potential intensity contributions from carbonyl C═O and from C−OH. At around 288.5 eV, we found that carboxyl COOH seems to be a major constituent of diesel soot, and we believe it is COOH that gives intensity in the ethylene spectra here as well. Most probably this structure is particularly prone to photochemical decomposition, in that decarboxylation under irradiation is a known phenomenon.[43] We disregard all other peaks for the following quantitative analysis, which is summarized in Table 3.

The area under either peak is considered proportional to the number of scatters or absorbers, which cause the peak (the molecular species). The area under the peaks for benzoquinone and graphite was divided by the total area under the NEXAFS spectrum and is listed in the columns "benzoquinone" and "graphitic" in Table 3. The sum of these relative intensities increases for samples 70 mm (0.300) to 20 mm (0.345), suggesting increasing graphitization of the samples. The ratio of these areas decreases for samples 70 to 20 mm, in line with the suggestion that the benzoquinone group density on the sample decreases as the surface decreases. A decrease of surface is expected with increasing graphitization.

Closer inspection of the peak at 292 eV reveals a slight shoulder, or edge, at about 291.2 eV. The spectrum of the 20-mm sampled soot, the most graphitized of the samples, shows the strongest shoulder or edge thus far. We identify this feature with the exciton of graphitic material. This is another confirmation that the sample from 20 mm is the more, or most, graphitized material among the three ethylene soot samples.

We have determined the size of the soot primary particles of the samples taken for NEXAFS study by sampling the ethylene/air diffusion flame according to a procedure described elsewhere.[35] At heights above the burner 20, 40, and 70 mm, along the flame axis, the primary particle size as determined by SEM is about 34, 47, and 55 nm (experimental uncertainty about 15%), respectively. The primary particle size shows a concave cap characteristic versus the sampling height.[35] Increasing sampling height means increasing residence time in a flame. Thus, primary particle size usually increases with residence times up to a plateau when the oxidation process balances surface growth.

What is normally anticipated is that the ratio of hydrogen to carbon is decreasing with increasing distance from the burner (i.e., a depletion of hydrogen by water formation, for instance). Also, with increasing distance from the burner, the ratio between oxygen and carbon increases, facilitating the oxidation of carbon and the readily formed particles.

We recall that with increasing height above the burner, the peak intensity at 285 eV decreases, the ratio of π- to σ-peak increases, and the surface-to-volume ratio increases. It was recently found for flame[14] and diesel soot[30] that the primary particles (i.e., the building bricks of soot fractal aggregates) do possess a relatively complex substructure. The primary particles

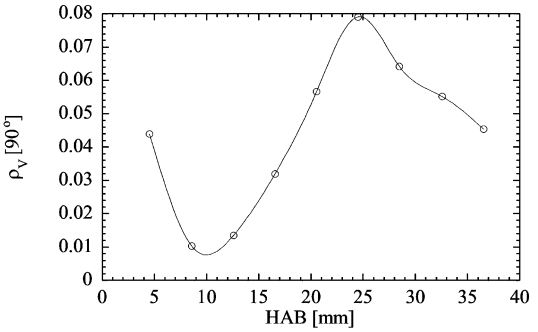

Figure 6. Vertical depolarization ratio at $\theta = 90°$ against HAB. Ethylene/air diffusion flame ($L_{flame} \approx 170$ mm, $v_{cold-gas} = 14.5$ cm/s, flow rate is 11 cm^3/s, air inlet of Bunsen burner is blocked). The abundance of BSUs (2−3 nm) corresponds to HAB less than 10 mm.

are typically around 20−50 nm in size and include subprimary particles of 5−8-nm size, which again contain elementary (basic structural) units, each formed by a 4-nm shell and a 2-nm nucleus.[14,30] The BSUs are believed to be formed by polymerization of aromatic rings through reactive coagulation mechanism[25,44] very close to the burner nozzle. With the presence of these nuclei, agglomeration into subprimary particles takes place at larger distances from the burner.[14,29,45] A possible mechanism is that the aromatic rings undergo polymerization and formation of BSUs and subprimary particles even at distances as large as 20 mm. These BSUs and subprimary particles have a relatively high crystallographic order, despite their small size. The subprimaries are then coated with surface layers of additional, partially polymerized aromatic rings. The "glue" that bonds the BSUs or subprimary particles and additional surface layers is carbon of lesser order, maybe amorphous carbon or hydrogen-containing carbonaceous matter. The overall order of the agglomerates decreases during this process. In addition, it is possible that the clusters react with oxygen, in particular because the region more distant from the burner is getting richer in oxygen. At 288.2 eV, the spectra of the soot particles sampled at 40 and 70 mm have a slightly peaked intensity; this feature is missing at the 20-mm sample. At this energy, carboxyl groups are typically observed.

The same spectroscopic observation is made on NEXAFS spectra of as-received and gas-phase oxidized glassy carbon samples. Upon oxidation, the glassy carbon spectrum shows an enhanced intensity at X-ray energies where the surface oxidic groups are expected (286.5−288.5 eV). Also, a slight decrease (about 5%) of the graphite peak at 285 eV is observed, accompanied by a remarkable broadening, likely due to benzoquinone-type species. Note that we make the same observations with the ethylene soot.

An additional confirmation for the presence of BSUs with higher short-range order on a small scale at shorter distances from the burner mouth comes from light scattering experiments. Depolarized visible light is very sensitive to short-range effects on small length scales.[36]

Figure 6 shows the depolarization ratio $\rho_V \equiv (I_{HV})/(I_{VV})$ (H and V stand for the linear polarization state, first and second footnote for scattered and incident light, respectively) of the light scattered by the soot at various heights above the burner mouth along the flame centerline. The steep increase of the depolarization for particles *larger* than 5 nm comes from *form*

(43) Smith, D. M.; Chughtai, A. R. *J. Atmos. Chem.* **1997**, *26*, 77−91.

(44) Siegmann, K.; Sattler, K.; Siegmann, H. C *J. Electron Spectrosc. Relat. Phenom.* **2002**, *126*, 191−202.

(45) Schnaiter, M.; Horvath, H.; Möhler, O.; Naumann, K.-H.; Saathoff, H.; Schöck, O. W. *J. Aerosol Sci.* **2003**, *34*, 1421−1444.

anisotropy effects, such as formation of chains and more complex clusters. The steep increase of depolarization for particles smaller than 5 nm can only be explained by ordering effects in these particles, the so-called *intrinsic anisotropy*.

As far as the significance of the above results to the general question relating the effect of different carbon aerosols on the global climate and radiative balance in the troposphere, it should be stressed that the optical properties of amorphous soot versus graphite-like materials are markedly different when absorption and scattering with UV−vis light are considered, as reported by several articles; see for instance Colbeck et al.[46,47] In particular, the imaginary part k of the soot complex refractive index $m = n + ik$ is reported to decrease with respect to the wavelength from the near UV up to the vis part of the spectrum (300 to 800 nm) in the range 0.8 to 0.35, according to different dispersion models reported in the literature,[19,20] computational schemes,[48] and experimental techniques.[49,50] In the case of graphite,[51] k shows a broad resonance peak at about 260 nm (∼4.8 eV). Moreover, the value of k at vis wavelengths is about 1.4 for graphite (i.e., about twice the value of soot at the same wavelengths). In fact, the major difference between graphite and soot is the hydrogen/carbon ratio, which is larger in the case of soot (for graphite without structural defects it would be zero). The increase of H/C reflects the decrease of free electrons Nc available for soot[21] with respect to the more stable, well-ordined, and conductive graphite microstructure. From the point of view of absorption, if Rayleigh regime is considered, namely particles with size parameter $x = \pi D/\lambda \ll 1$, a sensitivity analysis[52] shows that the absorption cross section at the same wavelength can vary by a factor 2, and therefore, an estimation of the volume fraction of particles from extinction measurements can be affected of a 100% error. On the other hand, spectral emissivity is significantly affected by a difference in the imaginary part of the refractive index, as we demonstrated in our previous work based on sensitivity analysis applied to a Drude−Lorentz dispersion model for soot optical constant.[5,21] Both spectral emissivity and single-scattering albedo, namely the ratio between scattering to extinction cross sections are relevant when the balance of radiative forcing in atmosphere is evaluated.[53]

4. Conclusions

Carbon K-edge NEXAFS was utilized to study the structure of Diesel soot, ethylene/air flame soot, carbon black, and graphite.

Comparison of the relative heights of C═C peak at 285 eV and exciton peak at about 291 eV permits us to make statements on the crystal order in the different types of soot (diesel, flame-generated, graphite) and at different heights above the burner z in a diffusion flame. Surprisingly, the presence of BSUs with graphitic microstructure is found at lower z distances in the flame. The structural analysis, in particular the graphitization degree, is performed by studying the core electron transitions at 285 and 292 eV. The ratio of the peak heights relative to the C═C π-peak at 285 eV and the σ-peak at 292 eV is used to quantify the degree of graphitization of the sample. The ratio is measured as 0.86, 0.73, and 0.91 for ethylene flame soot, diesel soot, and carbon black, respectively, with respect to 1.55 for graphite. Spectral signature of diesel soot differs from graphite and ethylene soot for the presence of peaks at 286 to 288.5 eV, which are attributed to phenol groups, aliphatic chains, and carboxyl groups. Graphite, diesel soot, and ethylene soot have in common the dip in the NEXAFS spectra at energies higher than 288 eV, which is absent in the case of carbon black owing to the larger presence in this last of C−H groups.

More careful analysis of ethylene soot spectrum reveals at 284 eV the presence of a pronounced intensity shoulder, which is attributed most probably to benzoquinone.

NEXAFS spectra of ethylene soot at different heights-above-burner show minute difference in intensity of the 285 eV π-peak and of corresponding 292 eV σ-peak. Ratio of π-peak to σ-peak intensity is found to decrease progressively from 20 to 40 to 70 mm. Moreover, the ratio between the integrated intensity of benzoquinone to graphite peaks was observed to increase for samples collected at 70 mm with respect to 20 mm, suggesting a decreasing of surface, which is consistent with a *higher* graphitization degree at the *lower* heights-above-burner z distances. This fact is interpreted, on the basis of previous literature,[14,30,54−56] as the presence of basic structural units or nuclei (∼2 nm) and subprimary particles (∼6 nm size) at lower z's, which, despite their small dimension, do exhibit higher short-range order on a small scale with respect to the larger primary particles (15−40 nm) and mature soot fractal aggregates. Depolarized light scattering on the ethylene/air diffusion flame at different z's is used as a tool to probe in situ the short-range effects on small scale. The steep increase of depolarization at z distances below 10 mm for particles smaller than 5 nm (subprimary particles) is explained in terms of intrinsic anisotropy consequent to ordering effect of their structure that was described in NEXAFS spectra as larger graphitization on a small scale.

Summarizing, it is evident that C(1s) NEXAFS spectroscopy is very helpful for the characterization of soot. In particular, it permits us not only to distinguish between soot material from different combustion sources, such as diesel engine soot versus ethylene burner soot, but also to assign molecular species that can be specific to the particular carbonaceous matter. This is important for combustion source attribution.

Moreover, NEXAFS spectra of ethylene soot generated closely or remotely from the burner nozzle show systematic differences, the interpretation of which can be supported by parallel investigations with light and small-angle X-ray scattering.[56] NEXAFS spectroscopy is thus useful for the formulation of combustion and soot formation scenarios.

The present results contribute to the comprehension of soot formation processes and to the speciation of different carbon fine powders on a microstructural basis. The discussed results are expected to be useful to the models implementing predictions of earth global warming in that soot aerosols with different levels

(46) Colbeck, I.; Hardman, E. J.; Harrison, R. M. *J. Aerosol Sci*. **1989**, *20*, 765−774.
(47) Vaglieco, B. M.; Beretta, F.; D'Alessio, A. *Combust. Flame* **1990**, *79*, 259−271.
(48) Chang, H.; Charalampopoluos, T. T. *Proc. R. Soc. London, Ser. A* **1990**, *430*, 577−591.
(49) Stagg, B. J.; Charalampopoluos, T. T. *Combust. Flame* **1993**, *94*, 381−396.
(50) Pluchino, A. B.; Goldberg, S. S.; Dowling, J. M.; Randall, C. M. *Appl. Opt*. **1980**, *19*, 3370−3372.
(51) Taft, E. A.; Philipp, H. R. *Phys. Rev*. **1965**, *138*, A197−A202.
(52) Ku, J. C.; Felske, J. D. *J. Quant. Spectrosc. Radiat. Transfer* **1984**, *31*, 569−574.
(53) Hottel, H. C.; Sarofim, A. F. *Radiative Transfer*; McGraw-Hill: New York, 1967.
(54) Wersborg, B. L.; Howard, J. B.; Williams, G. C. *Proc. Combust. Inst*. **1973**, *14*, 929−940.
(55) Howard, J. B.; Wersborg, B. L.; Williams, G. C. *Faraday Symp. Chem. Soc*. **1973** *7*, 109−119.
(56) di Stasio, S.; Mitchell, J. B. A.; LeGarrec, J. L.; Biennier, L.; Wulff, M. *Carbon* **2005**, in press.

of structure local order do behave differently with regard to UV sunlight absorption and to gas pollutants surface adsorption.

Acknowledgment. Financial support to one author (S. di Stasio) by MIUR-Italy, Projects FIRB No. RBAU01CXNP and FIRB No. RBAU01K749 and to the other author (A. Braun) by the National Science Foundation, Grant No. CHE-0891333 are gratefully acknowledged. We are indebted with S. B. Mun, BL 9.3, at the Advanced Light Source. The ALS is supported by the Director, Office of Science, Office of Basic Energy Sciences, Materials Sciences Division, of the U.S. Department of Energy under Contract No. DE-AC03-76SF00098 at Lawrence Berkeley National Laboratory.

EF058019G